Organic Process Research & Development **2003**, *7*, 942−950

Technology Reports

Modelling the Kinetics of a Reaction Involving a Sodium Salt of 1,2,4-Triazole and a Complex Substituted Aliphatic Halide

H. Grénman,[†] T. Salmi,*[,†] P. Mäki-Arvela,[†] J. Wärnå,[†] K. Eränen,[†] E. Tirronen,[‡] and A. Pehkonen[§]

Åbo Akademi, Process Chemistry Group, Laboratory of Industrial Chemistry, FIN-20500 Turku, Finland, Kemira Oyj, Espoo Research Center, P.O. Box 44, FIN-22071 Espoo, Finland, and Kemira Fine Chemicals Oy, P.O. Box 74, FIN-67101 Kokkola, Finland

Abstract:

A spontaneous reaction involving a sparingly soluble solid compound 1,2,4-triazole as sodium salt and a complex substituted aliphatic halide was studied. Kinetic experiments were performed in the temperature interval 120−170 °C. A part of the study was focused on the solubility of different compounds and the impact of triazole concentration on the reaction. On the basis of the experimental data, a mathematical model was developed, and the parameters in the model were estimated by nonlinear regression. On the basis of the consistency of the data, rather accurate values for the parameters were calculated from the experimental values and compared to the estimated ones. The model can be used as a helpful tool in developing industrial applications.

1. Introduction

Heterocyclic compounds have two or more different types of atoms in the ring structure. Carbon is the most common atom, but there is a vast number of other atoms that can join carbon in the ring. At least 13 million compounds can be found in *Chemical Abstracts* of which half are heterocyclic. Heterocyclic compounds play a significant role in nature, having a vital part in the metabolism of living cells. They are widely used in pharmacology, for example in the form of penicillin and morphine, but also for other purposes, such as pesticides, fungicides, herbicides, and insecticides.

Triazoles are heterocyclic compounds with three nitrogen and two carbon atoms. The main interest in triazoles lies in their pharmaceutical and agricultural applications. 1,2,4 -Triazole exists in a state of balance between form B1 and B2 (Figure 1). Theoretical calculations suggest that the form B1 dominates.[1−3] X-ray crystallographic and mass spectroscopic research support the calculations, even though the ratio varies.[4,5]

Figure 1. **Two different forms of 1,2,4-triazole, B1 and B2.**

The goal of this work was to research the kinetics of a reaction between a sodium salt of 1,2,4-triazole and a substituted aliphatic halide, where a product used in agriculture and an undesired byproduct is formed. Other alkylation reactions with 1,2,4-triazole have been investigated previously,[6,7] but to our knowledge no kinetic studies were performed. Knowledge of the kinetics is important for understanding the reaction mechanisms and optimising the production conditions. We performed experiments in a batch reactor at temperatures 120−170 °C. Focus was also given to solubility studies and researching the effect of different concentrations on reaction rates and selectivity.

The experimental data were used as a basis for developing a theoretical scheme (Figure 2) for the stoichiometry and mechanism of the reaction. In the scheme, A stands for the reactant (substituted aliphatic halide), P the desired main product, S the unwanted symmetric isomer of P, while C and T represent "cis" and "trans" isomers of different compounds. The notations "cis" and "trans" distinguish between structural forms where the substituent R_1 and the aliphatic carbon with associated substructure are either on the same or opposite side of the dioxolane ring. B1 and B2 denote the different forms of triazole.

2. Experimental Methods

2.1. Experimental Matrix. For the experimental research of the substitution reaction between the sodium salt of 1,2,4-triazole and the reactant (A), 15 experiments were performed where the temperature and concentrations varied. Temperature was the main parameter, and the concentrations were investigated only at temperatures of 142 and 170 °C to confirm that the concentration of triazole was high enough.

* Corresponding author. Fax: +358-2-2154479. E-mail: tapio.salmi@abo.fi.
† Abo Akademi.
‡ Kemira Oyj, Espoo Research Center.
§ Kemira Fine Chemicals Oy.

(1) Taft, R. W.; Anivia, F.; Taagepera, M.; Catalán, J.; Elguero, J. *J. Am. Chem. Soc*. **1986**, *108*, 3237.
(2) Ritchie, J. P. *J. Org. Chem*. **1989**, *54*, 3553.
(3) Cox, J. R.; Woodcock, S.; Hillier, I. H.; Vincent, M. A. *J. Phys. Chem*. **1990**, *94*, 5499.
(4) Deuschl, H. *Ber. Bunsen-Ges. Phys. Chem*. **1965**, *69*, 550.
(5) Goldstein, P.; Ladell, J.; Abowitz, G. *Acta Crystallogr., Sect. B*. **1969**, *25*, 135.
(6) Katritzky, A. R.; Kuzmierkiewicz, W.; Greenhill, V. *Recl. Trav. Chim. Pays-Bas* **1991**, *110*, 369.
(7) Begtrup, M.; Larsen, P. *Acta Chem. Scand*. **1990**, *44*, 1050.

Published on Web 09/20/2003
10.1021/op0300138 CCC: $25.00

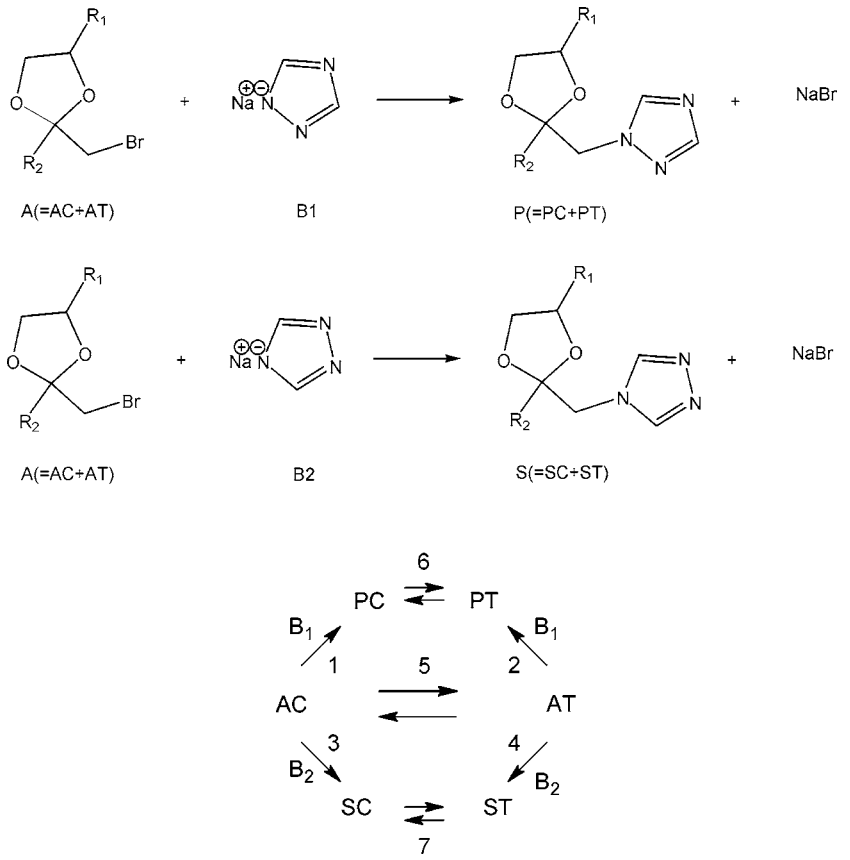

Figure 2. **Reaction schemes. The desidered product P is formed when triazole attaches to reactant A in form B1 and the unwanted product S is formed with form B2.**

Table 1. **Experimental matrix**

T (°C)	120	125	130	135	142	147	150	155	160	165	170
A, P, S	*	*	*	*	***	*	*	*	*	*	*
triazole	*				*		*		*		*
A, P, S (triazole over norm.)					*						*
potassium carbonate	*				*						*

The concentration of triazole in the liquid phase was researched at five temperatures, and the concentration of potassium carbonate (a base) in the liquid phase was researched at three temperatures. It was possible with these experiments to determine the temperature dependency of the reaction rate and the solubility of different components. Typically the reaction lasted 8 h (see Table 1.).

2.2. Equipment. The experiments were performed in a jacketed, isothermal reactor. The total volume of the batch reactor was 1000 mL of which 500 mL was used for the reaction mixture. The reactor was heated with circulating silicone oil. The experiments were performed under a nitrogen flow (AGA, 99.99%) to ensure that any irrelevant oxidation reactions would not affect the results. The outgoing nitrogen flow was cooled with a water cooler, and the flow was led through a bubble element filled with oil to ensure that no oxygen entered the system. The temperature was determined with a temperature probe attached to a PC. The temperature was recorded about 5 mm from the inner wall of the reactor and regulated manually. The heating lasted typically 25−50 min, and the variance in temperature, once the desired temperature was reached, was between 0.004 and 0.374 °C, depending on the experiment, and the highest temperature peak was 0.7 °C above the desired. The stirring in the reactor was very intense (propeller, impeller 400 rpm).

2.3. Experimental Procedure. The reactant (A) (∼6.5 × 10^{-4} mol/g), potassium carbonate (Merck), sodium salt of 1,2,4-triazole (commercial grade), and the polar aprotic solvent were weighed and charged into the reactor. The nitrogen flow was turned on and controlled with the bubble element. The reaction mixture was heated, and when the desired temperature was reached the first sample, which was the start point in the concentration profile, was taken. The reaction time was typically 8 h, and samples were withdrawn hourly. The temperature was kept constant during the experiment. The samples were taken with a 2-mL pipet upside down to ensure that the particles in the solid phase (triazole, K_2CO_3) were also taken in the sample. The samples for determining the concentration of triazole and potassium carbonate in the liquid phase were taken through a filter (7-μm pore size).

2.4. Analytical Apparatus. The chemical analyses were performed with a gas chromatograph (GC): HP 6890 with a HP-5 column (30 m × 0.32 mm, 0.25 μm film thickness) and a flame ionisation detector (FID). A liquid chromatograph (HPLC) HP-1100 with a LiChrosorb RP-18 column,

Table 2. **Chemicals used in the analysis.**

chemical	purity	producer
acetonitrile	>99.8%	Lab-Scan
dibutylamine	99%	Aldrich
phosphoric acid	85%	FF-Chemicals
hydrogen gas	99.999%	AGA
helium	99.999%	AGA
diethylphthalate (DEP)	99.3%	Merck

(length 250 mm, i.d. 4 mm, particle size 5 μm, and a UV detector) was also used for the analysis. Auto sampler systems were used in both chromatographs. Atom absorption spectroscopy (AAS) was also used in the analysis. The chemicals used are shown in Table 2.

2.5. Treatment of Samples. The samples, from which the progress of the reaction was determined, were weighed and diluted to 50 mL with acetonitrile. To the filtered samples, from which the concentration of triazole and potassium carbonate concentrations were determined, was added an aliquot of 5 mL of acetonitrile, after which the sample was diluted to 50 mL with ion-purified water.

Gas chromatography was used in the analysis of the reactions. The concentrations of the reactant (A) and the products (P and S) were analysed. The "cis"/"trans" forms of all three of the compounds were separated in the GC analysis. The possible enantiomers could not be separated with this GC method and were not investigated in this study. The method is described in detail in Table 3.

Liquid chromatography was used to determine the triazole concentrations in the liquid phase. The method is described in Table 4. DBA stands for dibutylamine, and the pH was set to 2.6 with orthophosphoric acid.

Atom absorption spectroscopy was used to determine the concentration of potassium carbonate in the liquid phase. The sample was diluted 100 times with ion-purified water. The apparatus was calibrated with solutions containing 0.5, 1, 2, and 5 ppm potassium and an amount of acetonitrile that was equivalent to the reaction liquid. Statistical analysis indicated that the calibration was successful ($R^2 = 0.9996$ in the beginning and $R^2 = 0.9991$ in the end).

3. Kinetic Results

The kinetic results will be discussed qualitatively in this section. The main factors are the effect of temperature and the concentration of the sodium salt of 1,2,4-triazole on the reaction rate and selectivity. According to the results, all of

Table 3. **Method used in gas chromatography**

column:	HP-5 (30 m × 0.32 mm, 0.25 μm film thickness)
gas:	He, inlet 0.965 bar, flow 2 mL/min
temperature program:	50 °C (3 min) → 30°C/min → 320°C (6 min) post time 320 °C (2 min)
detector:	FI, 280 °C
injection chaber:	250 °C
injector:	1 μL, automated, split injection, split ratio 20:1
integration:	ISTD, one point calibration
response factors:	
equation: $y = mx + b$, where y is area and x is amount	
DEP (inner standard):	$m = 1.00000$ and $b = 0.00000$
A (reactant):	$m = 6.93268 \times 10^{-1}$ and $b = 2.47641 \times 10^{-17}$
P (main product):	$m = 7.04418 \times 10^{-1}$ and $b = -4.68449 \times 10^{-17}$
S (P:s symmetric isomer):	$m = 7.00147 \times 10^{-1}$ and $b = -2.56403 \times 10^{-17}$

Table 4. **Method used in liquid chromatography**

Column:	LiCrosorb RP-18, length 250 mm, i.d. 4mm, patricle size 5 μm
Gradient:	A = 1 g DBA / 1 L H_2O, pH 2.6
	B = ACN (acetonitrile)

time (min)	A%	B%	flow (mL/min)
0.0	100	0	2.0
5.0	100	0	2.0
5.1	0	100	2.0
7.0	0	100	2.0
7.1	100	0	2.0
15.0	100	0	2.0

Detection:	UV, 200 nm
Injection:	10 μL
Integration:	ESTD, one point calibration

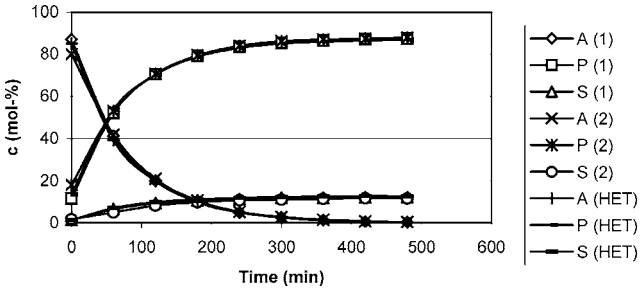

Figure 3. **Concentration of reactant A and products P and S as a function of time at 142 °C. The repeatability of the reaction is good. (HET = High excess triazole). Abbreviations from Figure 2.**

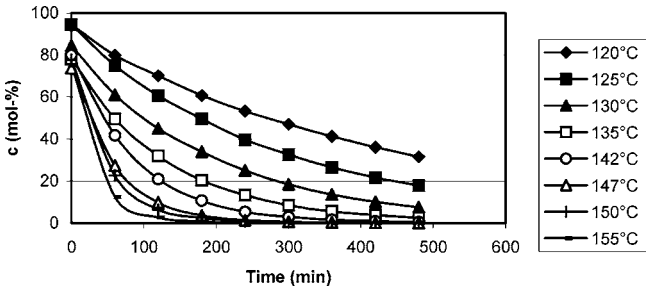

Figure 4. **Concentration of reactant (A) as a function of time at different temperatures.**

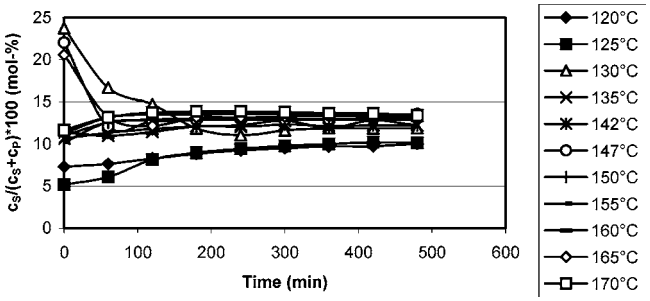

Figure 5. **Ratio of side product (S) as a function of time. Abbreviations from Figure 2.**

the reactant A reacted to products P and S. The difference in the sum of reagent and product concentrations in the beginning and the end of the experiment was on average 1.9%. The "cis"/"trans" ratio in the starting material was about 1.5, and the ratio of "cis"/"trans" isomers varied between 1.4 and 1.6 in the products. Traces of impurities were observed in the gas chromatographic analysis being maximally <1%. A typical kinetic experiment is displayed in Figure 3.

3.1. The Effect of Temperature on Reaction Rate and Selectivity. Temperature had a significant effect on the reaction rate. At the highest temperature (170 °C), the conversion was almost 100% after 1 h, while at the lowest temperature (120 °C), it was about 70% after 8 h. In Figure 4 we see the concentration of the reactant (A) as a function of reaction time is displayed for temperatures 120−155 °C.

Temperature had also an effect on the product selectivity. As revealed by Figure 5, the ratio of the side product S increased with temperature. In the beginning of the experiments, the ratio varied considerably due to experimental scattering caused by very low concentrations.

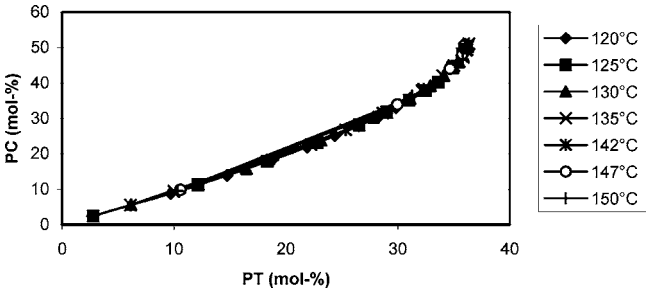

Figure 6. **Concentration of product P:s "cis" isomer (PC) as a function of the concentration of the "trans" isomer (PT). Abbreviations from Figure 2.**

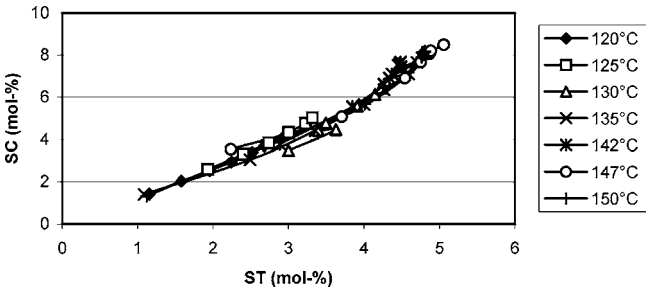

Figure 7. **Concentration of the side product S:s "cis" isomer (SC) as a function of the concentration of the "trans" isomer (ST). Abbreviations from Figure 2.**

As we notice from Figure 6, the reaction temperature had no significant effect on the selectivities of the stuctural isomers PT and PC. The ratio between the isomers is independent of the temperature; in other words, the "trans" and "cis" isomers of the reactant (A) reacted directly to "trans" and "cis" isomers of the product (P), and no variation in the ratio was observed. The "cis"/"trans" ratio was typically 1.4.

As demonstrated in Figure 7, the situation was analogous for the isomers of the side product S. The SC-to-ST ratio was typically 1.6.

3.2. The Effect of Triazole Concentration on Reaction Rate and Selectivity. The triazole concentration was a secondary parameter in the experimental study. The concentration was varied by increasing the amount of triazole in the reactor. It was first done at temperatures 142 and 170 °C with the same excess of triazole [triazole]/[A] = 1.850, and then the molar ratio was raised to 2.5.

In these experiments, no impact of the higher excess of triazole on the reaction rate was observed. As shown in Figure 8, the triazole concentration did not affect the reaction rate and selectivity. On the basis of these experiments, the concentration of triazole was concluded to be high enough, and thus, no further experiments were needed.

3.3. Solubility of the Sodium Salt of 1,2,4-Triazole and Potassium Carbonate in the Reaction Solvent. The solubility of triazole in the reaction mixture increased with temperature. The saturation concentrations of triazole varied from 0.03 to 0.04 mmol/mL within the temperature interval 120−170 °C in studies carried out with standard triazole amounts in the reaction mixture. In the experiments performed at 142 and 170 °C with a higher amount of triazole, the saturation concentrations varied between 0.04 and 0.05 mmol/mL, being somewhat higher than those determined for

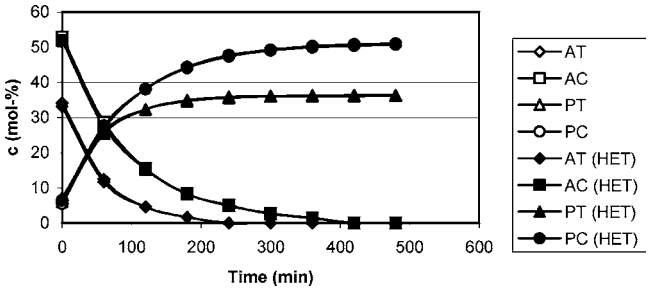

Figure 8. **Concentrations of reactants AT and AC and products PT and PC in experiments performed with two different triazole concentrations at 142 °C. (HET = High excess triazole, molar ratio 2.5). Abbreviations from Figure 2. Open symbol = normal concentration triazole, solid symbol = HET.**

standard concentrations. The variations in triazole concentrations did not affect the reaction rates (see Figure 8).The rise in solubility might well be explained by experimental deviation due to low concentrations and filtering. In the reaction mixture during the experiments there was an excess of triazole that caused saturation.

The solubility of potassium carbonate, was determined at 120, 142, and 170 °C. The saturation concentrations varied from 0.001 to 0.0023 mmol/mg, in such a way that the concentration decreased slightly during the reaction. The solubility increased with temperature (about 0.0007 mmol/mg from 120 to 170 °C). There was an excess of potassium carbonate in the reaction mixture during the experiments, causing saturation.

4. Kinetic Modelling

The quantitative treatment of experimental data was based on the reaction scheme displayed in Figure 2. The reaction scheme comprises the substitution reaction of the reagent isomers (AC and AT) with triazole as well as the isomerization of the reagents and products (PC and PT and SC and ST).

Two isomers of triazole (B1 and B2) coexist in the reaction mixture, but the isomerization reaction was assumed to be rapid enough to achieve a quasi-equilibrium B1 ⇌ B2 (reaction 8). This implies that the concentrations are related by $K_8 = c_{B2}/c_{B1}$, and c_{B2} can thus be expressed with c_{B1} exclusively.

The substitution reactions were taken to be essentially irreversible, whereas the isomerizations are reversible processes. The first attempt was thus to apply the single second-order kinetics on reactions 1−4 and reversible second-order kinetics on reactions 5−7. The rate expressions are seen below in eqs 1−7.

$$R_1 = k_1 c_{B1} c_{AC} \quad (1)$$

$$R_2 = k_2 c_{B1} c_{AT} \quad (2)$$

$$R_3 = k_3 c_{B2} c_{AC} \quad (3)$$

$$R_4 = k_4 c_{B2} c_{AT} \quad (4)$$

$$R_5 = k_5 (c_{AC} - c_{AT}/K_5) \quad (5)$$

$$R_6 = k_6 (c_{PC} - c_{PT}/K_6) \quad (6)$$

$$R_7 = k_7 (c_{SC} - c_{ST}/K_7) \quad (7)$$

The generation rates of the compounds are obtained from the general stoichiometric rule $r_i = \Sigma\, \nu_{ij} R_j$, where ν_{ij} denotes the stoichiometric coefficient of component i in reaction j. For the present case we get

$$r_{AC} = -R_1 - R_3 - R_5 \quad (8)$$

$$r_{AT} = -R_2 - R_4 + R_5 \quad (9)$$

$$r_{PC} = R_1 - R_6 \quad (10)$$

$$r_{PT} = R_2 + R_6 \quad (11)$$

$$r_{SC} = R_3 - R_7 \quad (12)$$

$$r_{ST} = R_4 + R_7 \quad (13)$$

Since the density of the reaction mixture was not known very precisely, the kinetic treatment was based on molar amounts per mass liquid i.e.

$$n_i = c_i m_L \quad (14)$$

Thus the concentrations have the unit mol/kg (= mmol/g).

For a completely back-mixed batch reactor, the mass balance of a component is written in the form

$$\frac{dn_i}{dt} = r_i m_L \quad (15)$$

A combination of eqs 14 and 15 gives

$$\frac{dc_i}{dt} = r_i \quad (16)$$

The mathematical model of the system (Figure 2) thus consists of eqs 8−13.

Since the concentration of triazole (B1 and B2) was practically constant during the reaction, all of the reactions become de facto pseudo-first order, and a rigorous analytical treatment is enabled. Further more, in the preliminary check of the kinetic data, the effect of the isomerization reactions was discarded ($R_5 = R_6 = R_7 = 0$). For instance, for the "cis" isomer (AC), the mass balance becomes after inserting the rate equation

$$\frac{dc_{AC}}{dt} = -(k_1 c_{B1} + k_3 c_{B2}) c_{AC} \quad (17)$$

By recalling that $c_{B2} = K_8 c_{B1}$ we, obtain

$$\frac{dc_{AC}}{dt} = -(k_1 + k_3 K_8) c_{B1} c_{AC} \quad (18)$$

which is easily integrated to

$$-\ln\left(\frac{c_{AC}}{c_{0AC}}\right) = (k_1 + k_3 K_8) c_{B1} t \quad (19)$$

For the "trans" isomer (AT) an analogous treatment gives

$$\frac{dc_{AT}}{dt} = -(k_2 + k_4 K_8) c_{B1} c_{AT} \quad (20)$$

$$-\ln\left(\frac{c_{AT}}{c_{0AT}}\right) = (k_2 + k_4 K_8) c_{B1} t \quad (21)$$

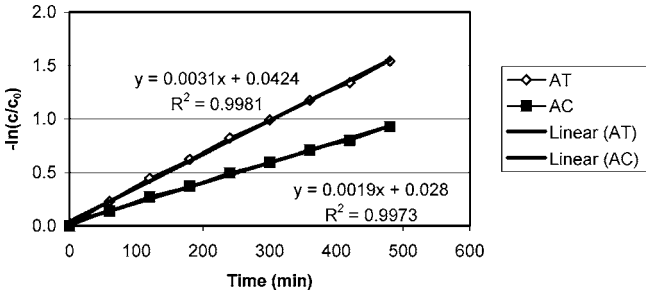

Figure 9. **$-\ln(c/c_0)$ for reagents AT and AC as a function of time at 120 °C. Abbreviations from Figure 2.**

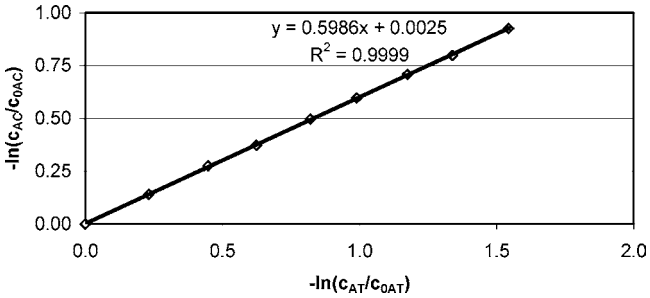

Figure 10. **$-\ln(c_{AC}/c_{0AC})$ as a function of $-\ln(c_{AT}/c_{0AT})$ at 120 °C. Abbreviations from Figure 2.**

Logarithmic test plots can now be prepared according to eqs 19 and 21. An example is displayed in Figure 9, which strongly suggests that the reactions are pseudo-first order with respect to the reagents.

All experimental data behaved in a similar way giving straight lines. Furthermore, a combination of the balance equations, of the reactions 19 and 20, gives a double logarithmic relation.

$$\frac{dc_{AC}}{dc_{AT}} = \left(\frac{k_1 + k_3K_8}{k_2 + k_4K_8}\right)\frac{c_{AC}}{c_{AT}} \tag{22}$$

A plot confirming this relation is displayed in Figure 10.

For the product PC, the balance equation becomes

$$\frac{dc_{PC}}{dt} = R_1 = k_1c_{B1}c_{AC} \tag{23}$$

$$\frac{dc_{PC}}{dt} = k_1c_{B1}c_{0AC}\, e^{-(k_1+k_3K_8)c_{B1}t} \tag{24}$$

which yields after integration

$$c_{PC} - c_{0PC} = \frac{k_1c_{B1}c_{0AC}}{\chi_1}(1 - e^{-\chi_1 t}) \tag{25}$$

where

$$\chi_1 = (k_1 + k_3K_8)c_{B1}$$

For the remaining products, an analogous approach is applied. The concentrations of PT, SC, and ST are obtained from relations

$$c_{PT} - c_{0PT} = \frac{k_2c_{B1}c_{0AT}}{\chi_2}(1 - e^{-\chi_2 t}) \tag{26}$$

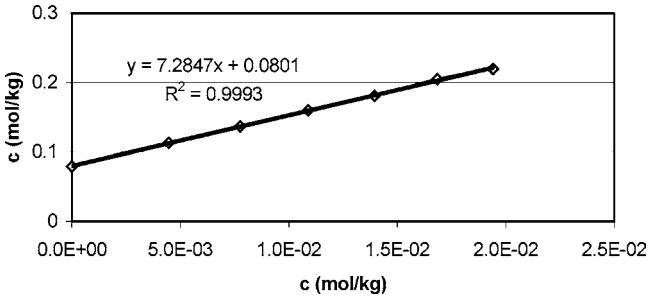

Figure 11. **Concentration of formed PC as a function of formed SC at 120 °C. Abbreviations from Figure 2.**

where

$$\chi_2 = (k_2 + k_4K_8)c_{B1}$$

$$c_{SC} - c_{0SC} = \frac{k_3K_8c_{B1}c_{0AC}}{\chi_3}(1 - e^{-\chi_3 t}) \tag{27}$$

$$\chi_3 = (k_1 + k_3K_8)c_{B1} = \chi_1$$

$$c_{ST} - c_{0ST} = \frac{k_4K_8c_{B1}c_{0AT}}{\chi_4}(1 - e^{-\chi_4 t}) \tag{28}$$

$$\chi_4 = (k_2 + k_4K_8)c_{B1} = \chi_2$$

A combination of eqs 1.24−1.26 and 1.25−1.27 gives relationships between the "cis" products (PC and SC) and "trans" products (PT and ST). The corresponding plots give straight lines for all experimental data. Some representative examples are shown in Figures 11 and 12. For instance, a combination of eqs 25 and 27 gives ($\chi_1 = \chi_3$)

$$\frac{c_{PC} - c_{0PC}}{c_{SC} - c_{0SC}} = \frac{k_1}{k_3K_8} = s_4 \tag{29}$$

$$\frac{c_{PT} - c_{0PT}}{c_{ST} - c_{0ST}} = \frac{k_2}{k_4K_8} = s_5 \tag{30}$$

where s denotes slope.

From the plots obtained at different temperatures the rate constants can be obtained as follows

$$k_1c_{B1} = \frac{s_1}{1 + \frac{1}{s_4}} \tag{31}$$

$$k_2c_{B1} = \frac{s_2}{1 + \frac{1}{s_5}} \tag{32}$$

$$k_3'c_{B1} = \frac{k_1c_{B1}}{s_4} \tag{33}$$

$$k_4'c_{B1} = \frac{k_2c_{B1}}{s_5} \tag{34}$$

where $k'_3 = k_3K_8$ and $k'_4 = k_4K_8$ and s stands for slope. The slopes are obtained: s_1 from eqs 19, s_2 from 21, s_3 from 22 (not used in the estimation), s_4 from 29 and s_5 from 30.

Table 5. **Results of the parameter estimation**

temp (°C)	k_1 (kg/mol·s)	std.rel.err. (%)	k_2 (kg/mol·s)	std.rel.err. (%)	k_3 (kg/mol·s)	std.rel.err. (%)	k_4 (kg/mol·s)	std.rel.err. (%)
120	1.94×10^{-3}	1.4	3.05×10^{-3}	2.0	1.66×10^{-4}	13.4	3.16×10^{-4}	12.9
125	2.63×10^{-3}	1.0	4.49×10^{-3}	1.5	3.00×10^{-4}	6.5	3.93×10^{-4}	9.7
130	3.73×10^{-3}	0.9	6.28×10^{-3}	1.5	6.48×10^{-4}	3.1	9.77×10^{-4}	4.6
135	5.27×10^{-3}	1.0	8.98×10^{-3}	2.1	8.51×10^{-4}	3.3	1.26×10^{-3}	5.5
142	9.01×10^{-3}	1.6	1.50×10^{-2}	3.2	1.42×10^{-3}	3.8	2.01×10^{-3}	6.4
147	1.10×10^{-2}	6.3	1.87×10^{-2}	14.3	1.77×10^{-3}	13.0	2.92×10^{-3}	23.2
150	1.52×10^{-2}	2.2	2.55×10^{-2}	5.1	2.28×10^{-3}	4.0	3.14×10^{-3}	8.2

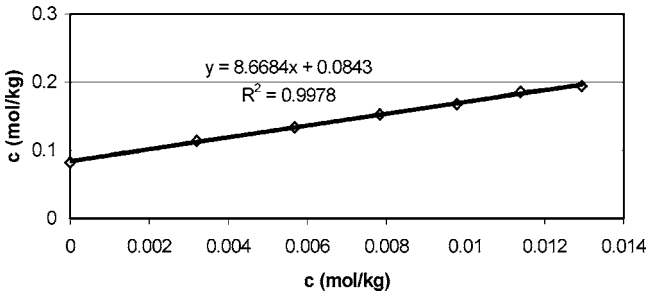

Figure 12. **Concentration of formed PT as a function of formed ST at the temperature 120 °C.**

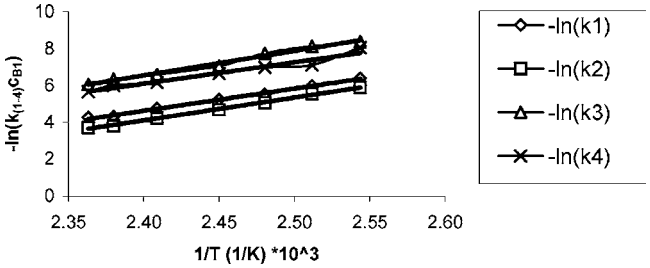

Figure 13. **Arrhenius plots for the different constants. $-\ln(k_j)$ as a function of $1/T$ (1/K).**

The next step is to check the temperature dependence of the rate parameters. Here the law of Arrhenius is used:

$$k_j c_{B1} = A_j \, e^{-E_{aj}/RT} \rightarrow \ln k_j c_{B1} = -\ln A_j + \frac{E_{a_j}}{RT} \qquad (35)$$

The Arrhenius plots for the different reactions are displayed in Figure 13 indicating that the description is adequate.

The rate parameters obtained from the test plots by linear regression were used as initial estimates in the final estimation of kinetic parameters by nonlinear regression. The regression analysis was based on the following objective function

$$Q = \sum_t \sum_i (c_{it\,\mathrm{exp}} - c_{it\,\mathrm{model}})^2 \qquad (36)$$

where all of the component concentrations were weighted equally. Since the first modelling attempt indicated that it is possible to neglect the effect of isomerization reactions 5, 6, and 7, they were excluded from the final analysis. The isomer ratio changed during the reaction, which indicates that isomerizations are slow, evidently very slow compared to the synthesis reactions.

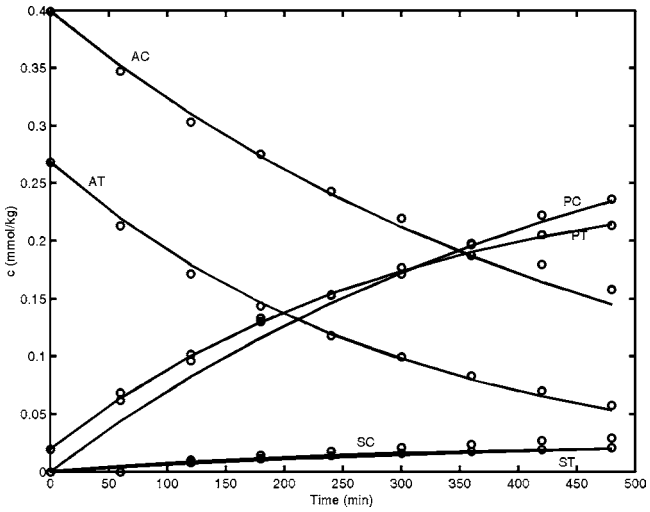

Figure 14. **Fit of the model to experimental data at 120 °C. The concentration of AC, AT, PC, PT, SC. and ST (mmol/g) as a function of the reaction time (min). Abbreviations from Figure 2.**

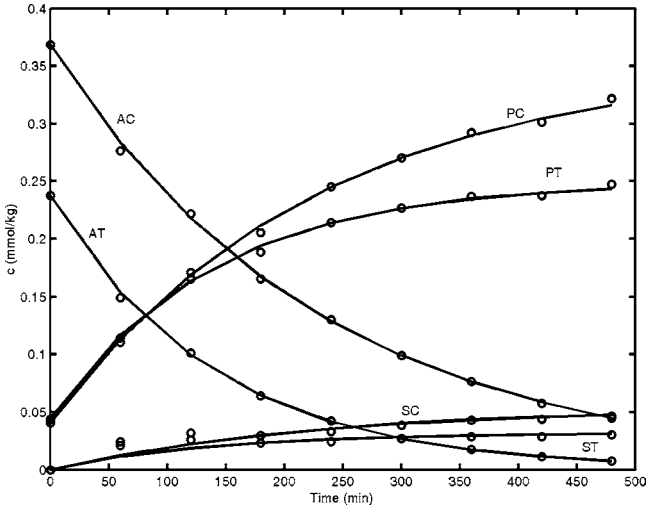

Figure 15. **Fit of the model to experimental data at 130 °C. The concentration of AC, AT, PC, PT, SC. and ST (mmol/g) as a function of the reaction time (min). Abbreviations from Figure 2.**

The objective function was minimised by a combined simplex−Levenberg−Marquardt algorithm.[8] The original differential equations 16 were solved numerically during the minimizations by a backward difference method[9] implemented in modelling software MODEST.[10] The following components were included in the parameter estimation: AC,

(8) Marquardt, D. W. *SIAM J.* **1963**, 431.

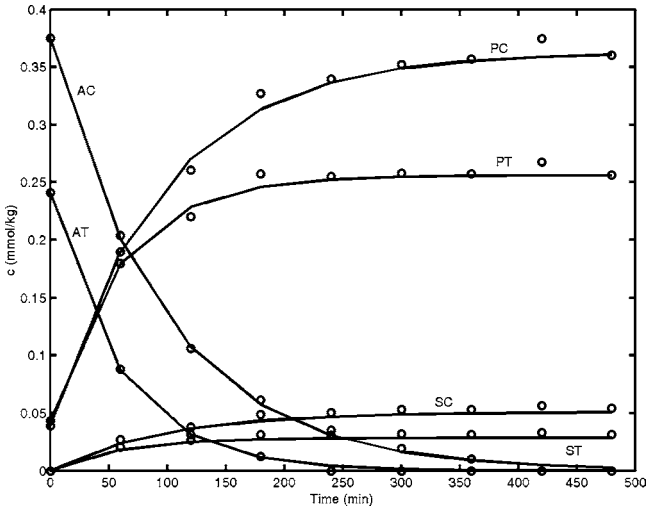

Figure 16. **Fit of the model to experimental data at 142 °C. The concentration of AC, AT, PC, PT, SC. and ST (mmol/g) as a function of the reaction time (min). Abbreviations from Figure 2.**

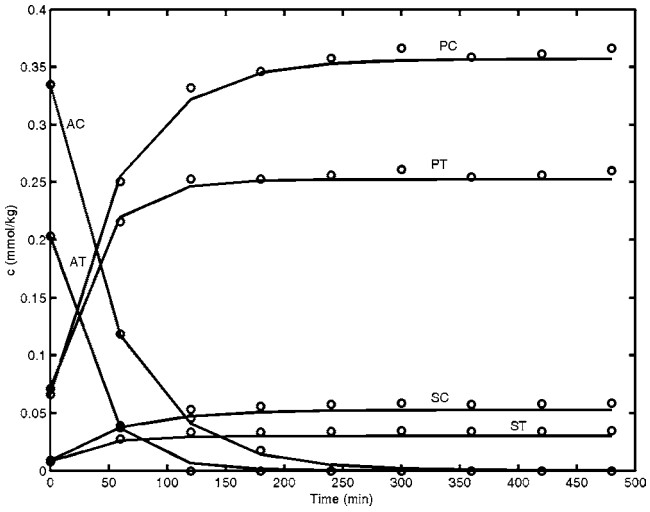

Figure 17. **Fit of the model to experimental data at 150 °C. The concentration of AC, AT, PC, PT, SC. and ST (mmol/g) as a function of the reaction time (min). Abbreviations from Figure 2.**

AT, PC, PT, SC, and ST. The estimated parameters were k_1, k_2, k_3, and k_4. A summery of parameter estimation results is provided in Table 5.

As shown by the Table, the estimation statistics are very good; the estimated relative standard error of the most important parameters being just few percent. Because of the high precision of the primary data, the parameter values obtained by linear regression were changed very little in the final nonlinear regression. A more illustrative view on the estimation is obtained by looking at fits of the model to experimental data (Figures 14−17).

In general we can conclude that the fit is excellent. No systematic deviations appear, and the model is able to follow the experimental trends at all temperatures investigated.

(9) Hindmarsh, A. C. *A Systematized Collection of ODE Solvers in Scientific Computing*; Stepleman, R., et al., Eds.; IMACS/North-Holland: Amsterdam, 1983; pp 55−64.

(10) Haario, H. *MODEST-Users's Guide*; Profmath Oy: Helsinki, 1994.

Table 6. **Activation energy and frequency factor calculated with the help of the estimated parameters in Table 5**

	A (min^{-1}) (mean value)	E_a (kJ/mol)
k_1c_{B1}	5.8183×10^9	94.023
k_2c_{B1}	1.5909×10^{10}	95.694
k_3c_{B1}	5.2341×10^{11}	115.947
k_4c_{B1}	1.6928×10^{11}	110.717

Furthermore, the good fit suggests that the model is sufficiently sophisticated and there is no need to include additional features, such as the isomerization rates (reactions 5, 6, and 7 in Figure 1). The Arrhenius parameters (eq 35) are calculated with the help of the rate constants presented in Table 5. A summary of the preexponential factors is provided in Table 6.

The activation energies E_{a1} and E_{a2} are almost equal which is in accordance with primary data; the ratio of PC and PT was independent of the temperature. We can conclude almost the same for E_{a3} and E_{a4} (SC and ST).

5. Conclusions

The kinetics of a reaction involving a sodium salt of 1,2,4-triazole and a substituted aliphatic halide was investigated in a batch reactor. A quantitative analysis of the reaction components revealed that the reaction liquid was saturated by the dissolved solid, which allowed a simplified treatment of data. A theoretical reaction scheme (Figure 2) was proposed and used as a basis for estimation of temperature-dependent kinetic parameters. The isomerization steps included in the scheme turned out to be negligible for kinetics. The stepwise procedure was successful in parameter estimation, giving finally a kinetic model which is a useful tool in process scale-up and optimisation.

Notation

A	frequency factor
A	reactant (substituted aliphatic halide)
AC	"cis" isomer of reagent A (Figure 2)
AT	"trans" isomer of reagent A (Figure 2)
B1	triazole form (Figure 1)
B2	triazole form (Figure 1)
c	concentration (mmol/g = mol/kg), (mainly in the modelling section) or as (mol %) of the sum of reagent A and products P&S (mainly in the kinetic results section)
E_a	activation energy
K	c_{B2}/c_{B1}
k	rate constant
m_i	mass
n	amount of substance
P	main product
PC	"cis" isomer of product P (Figure 2)
PT	"trans" isomer of product P (Figure 2)
Q	objective function in regression
R	gas constant

R	reaction rate
S	side product (symmetric isomer)
SC	"cis" isomer of product S (Figure 2)
ST	"trans" isomer of product S (Figure 2)
r	generation rate
T	temperature
T	"trans" isomer
t	time
ν_{ij}	stoichiometric coefficient of component i in reaction j.
$\chi_1 = \chi_3$	$(k_1+k_3K_8)c_{B1}$
$\chi_2 = \chi_4$	$(k_2+k_4K_8)c_{B1}$

Subscripts and superscripts

i	component
j	reaction
l	liquid phase
0	initial quantity or concentration

Abbreviations

AAS	atom absorption spectroscopy
ACN	acetonitrile
DBA	dibutylamine
DEP	diethylphthalate
FID	flame ionisation detector
GC	gas chromatograph
HPLC	liquid chromatograph
i.d.	inner diameter
ppm	parts per million
rpm	revolutions per minute
UV	ultraviolet
s	slope
HET	high excess triazole

Acknowledgment

This work is a part of the activities at Åbo Akademi Process Chemistry Group within the Finnish Centre of Excellence Program (2000−2005) by the Academy of Finland. Financial support from Kemira is gratefully acknowledged.

Received for review March 29, 2003.

OP0300138